Processed seismic data and ERT inversion models used in the estimation of injected masses for the Ketzin CO2 pilot project for the years 2009 and 2012

(https://doi.org/will be provided)

Wolfgang Weinzierl, Merlin Ganzer, Dennis Rippe, Stefan Lüth, Cornelia Schmidt-Hattenberger

GFZ German Research Centre for Geosciences, Potsdam, Germany

1. Licence

2. Citation

When using the data please cite:

Weinzierl, W.; Ganzer, M.; Rippe, D.; Lüth, S. Schmidt-Hattenberger, C. (2021): Processed seismic data and ERT inversion models used in the estimation of injected masses for the Ketzin CO2 pilot project for the years 2009 and 2012. GFZ Data Services. https://doi.org/10.5880/GFZ.4.8.2021.004

Table of contents

3. Data Description

3.1. Sampling method

Seismic: Seismic data was acquired in 2009 and 2012. Coordinates are provided in a custom CRS derived from WGS84-UTM32. Coordinates are provided in km. Translation into WGS-UTM32 can be done accordingly:

- Y-Coordinate: Multiply by 1000 to map to meter
- X-Coordinate: Multiply by 1000 and subtract 3000000 to map to meter

This translates the coordinates to WGS-UTM32.

ERT: ERT data was acquired in 2009 and 2012. The inversion domain is spanned by three boreholes KTZ200-201-202, with relative coordinates from KTZ200 x,y= (0,0).

The coordinates of the boreholes in WGS84-UTM32 are following:

- KTZ200: x,y=(355292.7,5817801.6)
- KTZ201: x,y=(355242.7,5817803.7)
- KTZ202: x,y=(355296.8,5817901.4)

3.2.Analytical procedure:

Seismic and geoelectric/electro-magnetic methods are used as complementary tools for the identification of fluid/gas effects in underground storage and production scenarios. Both methods generally have very different resolution. Seismic tends to be acquired by much more dense geometrical layouts and the geoelectric or electro-magnetic acquisition being a potential field method shows information integrated over spatial distances. These inherent scale and design dependent differences require spatial tuning in joint inversion approaches and careful matching in independent interpretations of both methods. The provided data is a collection of results matching seismic and electrical resistivity tomography (ERT) from two repeat surveys acquired during CO2 storage operations at the Ketzin pilot site in Germany. Volumes of injected mass are obtained from the averaged acoustic impedance change (seismic) in the vicinity of the injection well and compared to volumes inferred from the ERT cross-well acquisition.

3.3.Data processing

Seismic – Processing – Previous work - Ivanova et al. 2012 and Ivandic et al. 2015

Results are following the more recent estimations from Ivandic et al. 2015. Parameters used in mass estimation are listed in Table 1. The estimated mass of the seismic acquisition

$$M_{CO2} = \sum_N \phi \, S_{CO2} \, \rho \, dxdy \, H$$

is computed according to the following assumptions:

- ϕ is the porosity of the reservoir assume to be the same in all CDP bins (the average value of porosity is taken from Forster et al. 2010)

- S_{CO2} is the CO_2 saturation in the reservoir taken from the PNG minimum and maximum gas saturation scenarios
- ρ is the CO_2 density derived using the monitored pressure and temperature conditions in the reservoir
- dx and dy define the size of one CDP bin
- N is the total number of CDPs
- H is the thickness of the part of the reservoir containing CO_2

The thickness of the layer containing CO_2, H, is derived from the velocity push-down effect, DT, using the following relation:

$$H=\Delta T/2\ (1/V2 - 1/V1)$$

Velocities are derived from a petrophysical investigation which resulted in a linear dependence of saturated compressional with increasing saturations.

$$V2 = -0.46\ Sg\ V1$$

<table>
<tr><td>Φ</td><td colspan="4">0.2</td></tr>
<tr><td rowspan="5">S_{CO2}</td><td colspan="2">2009</td><td colspan="2">2012</td></tr>
<tr><td>Amplitude diff.</td><td>Sg</td><td>Amplitude diff.</td><td>Sg</td></tr>
<tr><td>0.3–0.46</td><td>0.474</td><td>0.3–0.48</td><td>0.560</td></tr>
<tr><td>0.46–0.7</td><td>0.381</td><td>0.48–0.6</td><td>0.580</td></tr>
<tr><td>0.7–1.0</td><td>0.405</td><td>0.6–1.0</td><td>0.387</td></tr>
<tr><td rowspan="3">ρ</td><td colspan="2">2009</td><td colspan="2">2012</td></tr>
<tr><td colspan="2">266.62 kg/m^3</td><td colspan="2">215 kg/m^3</td></tr>
<tr><td colspan="4"></td></tr>
<tr><td>dx/dy</td><td colspan="4">12.5m/12.5m</td></tr>
</table>

Table 1: Parameters used in the estimation of mass from timelapse seismic following Ivandic et al. 2015 for Repeat 2009 and 2012.

ERT – Processing

The ERT inversion was performed using the ERT lab software which works in an unstructured grid domain. The results of the 3D crosswell inversion were subsequently regridded into a structured grid domain. The depth range of investigation was limited to the range [-620,-650].

Figure 5 shows the filtered raw and regridded resistivity values form the inversions for repeat surveys in 2009 and 2012. The minor differences can be explained by the nearest neighboring algorithm used to populate the structured grid with the unstructured raw inversion results.

The resistivity models obtained by the tomography are used to evaluate saturations given the Archie equation. Using the saturation exponent n as well as the background resistivity R0 of the fully brine saturated medium saturations can be computed according to following relation:

$$S_{CO2} = 1 - (R_0/\text{Resistivity})^{1/n}$$

With saturations, porosities ϕ, densities ρ and volumes defined by grid cell sizes (dx,dy,dz), mass estimation can be performed:

$$M_{CO2} = \sum_N \phi \, S_{CO2} \, \rho \, dx \, dy \, dz$$

Default parameters used in the mass estimates were following:

$$n = 1.62$$

$$R_0 = 0.725$$

$$\phi = 0.2$$

4. File description

4.1.File: 2021-004_Ketzin_Seis_ERT_DataShare.hdf5

General: Processed seismic data and ERT inversion models used in the estimation of injected masses for the Ketzin CO2 pilot project for the years 2009 and 2012.

Datasets are grouped in different levels. Two main levels exist. Raw data includes processed seismic data and ERT inversion results. Seismic mass estimation relies on amplitude differences and timeshifts. ERT inversion results have been converted from VTK. Deatils are listed in Table 2.

Raw

- Seismic
  - 2009: Two datasets for Amplitude differences and Timeshifts
  - 2012: Two datasets for Amplitude differences and Timeshifts
- ERT
  - 2009: One dataset with [x,y,z,Resistivity,Volume,Active]
  - 2012: One dataset with [x,y,z,Resistivity,Volume,Active]

Processed

- Seismic
  - Mass_2009
  - Mass_2012
- ERT
  - Gridded_2009
  - Gridded_2012
    - Seismic_ERT_Mesh_1x1
    - Seismic_ERT_Mesh_1x1_CDP_Adjusted_6.25m
    - Seismic_ERT_Mesh_1x1_CDP_Adjusted_12.5m

Contents of the datasets present in the individual groups is explained in Table 1. Below is a short description of the raw data processing (ERT) and columns present in the datasets.

Raw data - ERT Processing

- Convert ERTLab to VTK
- Write cell centers to dataset
    - x – Cell center x
    - y – Cell center y
    - z – Cell center z
    - Resistivity – Cell center resistivities
    - Volume – Cell center volumes
    - Active – Cell center identifier for inversion region (1) and boundary region (0)

Raw data – Seismic

- Amplitude differences between baseline and monitor
    - x – CDP center x
    - y – CDP center y
    - dA – CDP center Amplitude difference
- Timeshifts between baseline and monitor
    - x – CDP center x
    - y – CDP center y
    - IL – Inline number
    - XL – Crossline number
    - Lower – CDP center lower window timeshift
    - Upper – CDP center upper window timeshift
    - Timeshift – CDP center timeshift

Dataset Identifier	Level	Size	Size Description	Explanation	Data content
/Processed	Group			Processed data Group	
/Processed/ERT	Group			Processed ERT Data	ERT Domain: -50<x<0 / 0<y<100 / 645<z<625 [m]
/Processed/ERT/Gridded_2009	Group			Structured grid for ERT results 2009	
/Processed/ERT/Gridded_2009/resistivity	Dataset	{19;34;31}	nx,ny,nz	Resampled cell resistivity	
/Processed/ERT/Gridded_2009/volume	Dataset	{19;34;31}	nx,ny,nz	Resampled cell volume	
/Processed/ERT/Gridded_2009/x_grid	Dataset	{34;19}	ny,nx	X values gridded	
/Processed/ERT/Gridded_2009/x_unique	Dataset	{19}	nx	X vector unique values	
/Processed/ERT/Gridded_2009/y_grid	Dataset	{34;19}	ny,nx	Y values gridded	
/Processed/ERT/Gridded_2009/y_unique	Dataset	{34}	ny	Y vector unique values	
/Processed/ERT/Gridded_2009/z_unique	Dataset	{31}	nz	Z vector unique values	
/Processed/ERT/Gridded_2012	Group			Structured grid for ERT results 2012	
/Processed/ERT/Gridded_2012/resistivity	Dataset	{19;34;31}	nx,ny,nz	Resampled cell resistivity	
/Processed/ERT/Gridded_2012/volume	Dataset	{19;34;31}	nx,ny,nz	Resampled cell volume	
/Processed/ERT/Gridded_2012/x_grid	Dataset	{34;19}	ny,nx	X values gridded	
/Processed/ERT/Gridded_2012/x_unique	Dataset	{19}	nx	X vector unique values	
/Processed/ERT/Gridded_2012/y_grid	Dataset	{34;19}	ny,nx	Y values gridded	
/Processed/ERT/Gridded_2012/y_unique	Dataset	{34}	ny	Y vector unique values	
/Processed/ERT/Gridded_2012/z_unique	Dataset	{31}	nz	Z vector unique values	
/Processed/Seismic	Group			Processed Seismic Data	Seismic Domain: x and y in UTM [km]
/Processed/Seismic/2009_AmpDiff	Dataset	{321;281}	ny,nx	Relative amplitude difference 2009	
/Processed/Seismic/2009_TimeShift	Dataset	{321;281}	ny,nx	Timeshifts 2009	
/Processed/Seismic/2012_AmpDiff	Dataset	{321;281}	ny,nx	Relative amplitude difference 2012	
/Processed/Seismic/2012_TimeShift	Dataset	{321;281}	ny,nx	Timeshifts 2012	
/Processed/Seismic/Mass_2009	Group			Mass estimation 2009	
/Processed/Seismic/Mass_2009/H	Dataset	{321;281}	ny,nx	Thickness	
/Processed/Seismic/Mass_2009/Mass	Dataset	{321;281}	ny,nx	Mass	
/Processed/Seismic/Mass_2009/Sg	Dataset	{321;281}	ny,nx	CO2 saturations	
/Processed/Seismic/Mass_2009/V0	Dataset	{321;281}	ny,nx	Vp fully brine saturated	
/Processed/Seismic/Mass_2009/V1	Dataset	{321;281}	ny,nx	Vp gas saturated	
/Processed/Seismic/Mass_2009/dA	Dataset	{321;281}	ny,nx	Relative amplitude difference	
/Processed/Seismic/Mass_2009/dT	Dataset	{321;281}	ny,nx	Timeshifts	
/Processed/Seismic/Mass_2012	Group			Mass estimation 2009	
/Processed/Seismic/Mass_2012/H	Dataset	{321;281}	ny,nx	Thickness	
/Processed/Seismic/Mass_2012/Mass	Dataset	{321;281}	ny,nx	Mass	
/Processed/Seismic/Mass_2012/Sg	Dataset	{321;281}	ny,nx	CO2 saturations	
/Processed/Seismic/Mass_2012/V0	Dataset	{321;281}	ny,nx	Vp fully brine saturated	
/Processed/Seismic/Mass_2012/V1	Dataset	{321;281}	ny,nx	Vp gas saturated	
/Processed/Seismic/Mass_2012/dA	Dataset	{321;281}	ny,nx	Relative amplitude difference	
/Processed/Seismic/Mass_2012/dT	Dataset	{321;281}	ny,nx	Timeshifts	
/Processed/Seismic/bool_seis_acquisition	Dataset	{321;281}	ny,nx	Bool to identify Acquisition area	

Table 2: Contents of the file for the mass estimation from processed seismic data and ERT inversion results.

/Processed/Seismic/bool_seis_ert_overlap	Dataset	{321;281}	ny,nx	Bool to identify ERT overlap	
/Processed/Seismic/x_grid	Dataset	{321;281}	ny,nx	X values gridded	
/Processed/Seismic/x_unique	Dataset	{281}	nx	X vector unique values	
/Processed/Seismic/y_grid	Dataset	{321;281}	ny,nx	Y values gridded	
/Processed/Seismic/y_unique	Dataset	{321}	ny	Y vector unique values	
/Processed/Seismic_ERT_Mesh_1x1	Group			Mass estimation – 1x1m Grid resampled Original overlap with ERT	
/Processed/Seismic_ERT_Mesh_1x1/2009_AmpDiff	Dataset	{122;75}	ny,nx	Relative amplitude difference – 2009	
/Processed/Seismic_ERT_Mesh_1x1/2009_	Dataset	{122;75}	ny,nx	Thickness – 2009	
/Processed/Seismic_ERT_Mesh_1x1/2009_	Dataset	{122;75}	ny,nx	Mass – 2009	
/Processed/Seismic_ERT_Mesh_1x1/2012_AmpDiff	Dataset	{122;75}	ny,nx	Relative amplitude difference – 2012	
/Processed/Seismic_ERT_Mesh_1x1/2012_	Dataset	{122;75}	ny,nx	Thickness – 2012	
/Processed/Seismic_ERT_Mesh_1x1/2012_	Dataset	{122;75}	ny,nx	Mass – 2012	
/Processed/Seismic_ERT_Mesh_1x1/bool_seis_ert_overlap	Dataset	{122;75}	ny,nx	Bool to identify ERT overlap	
/Processed/Seismic_ERT_Mesh_1x1/x_grid	Dataset	{122;75}	ny,nx	X values gridded	
/Processed/Seismic_ERT_Mesh_1x1/y_grid	Dataset	{122;75}	ny,nx	Y values gridded	
/Processed/Seismic_ERT_Mesh_1x1_CDP_Adjusted_12.5m	Group			Mass estimation – 1x1m Grid resampled Original overlap with ERT + CDP	
/Processed/Seismic_ERT_Mesh_1x1_CDP_Adjusted_12.5m/2009_AmpDiff	Dataset	{227;179}	ny,nx	Relative amplitude difference – 2009	
/Processed/Seismic_ERT_Mesh_1x1_CDP_Adjusted_12.5m/2009_H	Dataset	{227;179}	ny,nx	Thickness – 2009	
/Processed/Seismic_ERT_Mesh_1x1_CDP_Adjusted_12.5m/2009_Mass	Dataset	{227;179}	ny,nx	Mass – 2009	
/Processed/Seismic_ERT_Mesh_1x1_CDP_Adjusted_12.5m/2012_AmpDiff	Dataset	{227;179}	ny,nx	Relative amplitude difference – 2012	
/Processed/Seismic_ERT_Mesh_1x1_CDP_Adjusted_12.5m/2012_H	Dataset	{227;179}	ny,nx	Thickness – 2012	
/Processed/Seismic_ERT_Mesh_1x1_CDP_Adjusted_12.5m/2012_Mass	Dataset	{227;179}	ny,nx	Mass – 2012	
/Processed/Seismic_ERT_Mesh_1x1_CDP_Adjusted_12.5m/bool_seis_ert_overlap	Dataset	{227;179}	ny,nx	Bool to identify ERT overlap	
/Processed/Seismic_ERT_Mesh_1x1_CDP_Adjusted_12.5m/x_grid	Dataset	{227;179}	ny,nx	X values gridded	
/Processed/Seismic_ERT_Mesh_1x1_CDP_Adjusted_12.5m/y_grid	Dataset	{227;179}	ny,nx	Y values gridded	
/Processed/Seismic_ERT_Mesh_1x1_CDP_Adjusted_6.25m	Group			Mass estimation – 1x1m Grid resampled Original overlap with ERT + ½ CDP	
/Processed/Seismic_ERT_Mesh_1x1_CDP_Adjusted_6.25m/2009_AmpDiff	Dataset	{215;167}	ny,nx	Relative amplitude difference – 2009	

Table 2 (continued)

/Processed/Seismic_ERT_Mesh_1x1_CDP_Adjusted_6.25m/2009_H	Dataset	{215;167}	ny,nx	Thickness – 2009	
/Processed/Seismic_ERT_Mesh_1x1_CDP_Adjusted_6.25m/2009_Mass	Dataset	{215;167}	ny,nx	Mass – 2009	
/Processed/Seismic_ERT_Mesh_1x1_CDP_Adjusted_6.25m/2012_AmpDiff	Dataset	{215;167}	ny,nx	Relative amplitude difference – 2012	
/Processed/Seismic_ERT_Mesh_1x1_CDP_Adjusted_6.25m/2012_H	Dataset	{215;167}	ny,nx	Thickness – 2012	
/Processed/Seismic_ERT_Mesh_1x1_CDP_Adjusted_6.25m/2012_Mass	Dataset	{215;167}	ny,nx	Mass – 2012	
/Processed/Seismic_ERT_Mesh_1x1_CDP_Adjusted_6.25m/bool_seis_ert_overlap	Dataset	{215;167}	ny,nx	Bool to identify ERT overlap	
/Processed/Seismic_ERT_Mesh_1x1_CDP_Adjusted_6.25m/x_grid	Dataset	{215;167}	ny,nx	X values gridded	
/Processed/Seismic_ERT_Mesh_1x1_CDP_Adjusted_6.25m/y_grid	Dataset	{215;167}	ny,nx	Y values gridded	
/Raw	**Group**			**Raw data Group**	
/Raw/ERT	Group			Raw ERT data	
/Raw/ERT/2009_ERT	Dataset	{105820;6}		VTK data exported 2009	x,y,z,Resistivity,Volume,Active
/Raw/ERT/2012_ERT	Dataset	{105820;6}		VTK data exported 2012	x,y,z,Resistivity,Volume,Active
/Raw/Seismic	Group			Raw Seismic data	
/Raw/Seismic/2009_AmpDiff	Dataset	{90201;3}		Relative amplitude difference 2009	x,y,Amplitude difference
/Raw/Seismic/2009_TimeShift	Dataset	{44389;7}		Timeshifts 2009	x,y,Inline,Xline,Upper window dT, Lower window dT, Timeshift=Upper-Lower
/Raw/Seismic/2012_AmpDiff	Dataset	{144761;3}		Relative amplitude difference 2012	x,y,Amplitude difference
/Raw/Seismic/2012_TimeShift	Dataset	{44389;7}		Timeshifts 2012	x,y,Inline,Xline,Upper window dT, Lower window dT, Timeshift=Upper-Lower

Table 2 (continued)

4.2.File: Ketzin_Seis_ERT_DataShare_Masses.csv

General: Estimated masses for the processed seismic data and ERT inversion models.

Masses are obtained for increasing thickness (H) threshold for the seismic and decreasing zone thicknesses for the ERT inversion models. For the seismic estimation, three inspection areas (AOI) are considered. For the ERT estimation, sensitivities on the background resistivity R0 and cementation exponent n are considered (see Figure 1). The file consists of the following 20 columns:

1. Line number
2. Seismic thickness threshold
3. ERT zone thickness centered around z=-635m

2009 – Results for repeat survey

4. Seismic mass – AOI defined by injector and monitoring boreholes
5. Seismic mass – AOI defined by injector and monitoring boreholes + ½ CDP bin size
6. Seismic mass – AOI defined by injector and monitoring boreholes + 1 CDP bin size
7. ERT mass – Background resistivity R0 = 0.725 / Cementation exponent n = 1.62
8. ERT mass – Background resistivity R0 = 0.700 / Cementation exponent n = 1.62
9. ERT mass – Background resistivity R0 = 0.650 / Cementation exponent n = 1.62
10. ERT mass – Background resistivity R0 = 0.725 / Cementation exponent n = 1.62
11. ERT mass – Background resistivity R0 = 0.725 / Cementation exponent n = 1.20
12. ERT mass – Background resistivity R0 = 0.725 / Cementation exponent n = 1.10

2012 – Results for repeat survey

13. Seismic mass – AOI defined by injector and monitoring boreholes
14. Seismic mass – AOI defined by injector and monitoring boreholes + ½ CDP bin size
15. Seismic mass – AOI defined by injector and monitoring boreholes + 1 CDP bin size
16. ERT mass – Background resistivity R0 = 0.725 / Cementation exponent n = 1.62
17. ERT mass – Background resistivity R0 = 0.700 / Cementation exponent n = 1.62
18. ERT mass – Background resistivity R0 = 0.650 / Cementation exponent n = 1.62
19. ERT mass – Background resistivity R0 = 0.725 / Cementation exponent n = 1.62
20. ERT mass – Background resistivity R0 = 0.725 / Cementation exponent n = 1.20
21. ERT mass – Background resistivity R0 = 0.725 / Cementation exponent n = 1.10

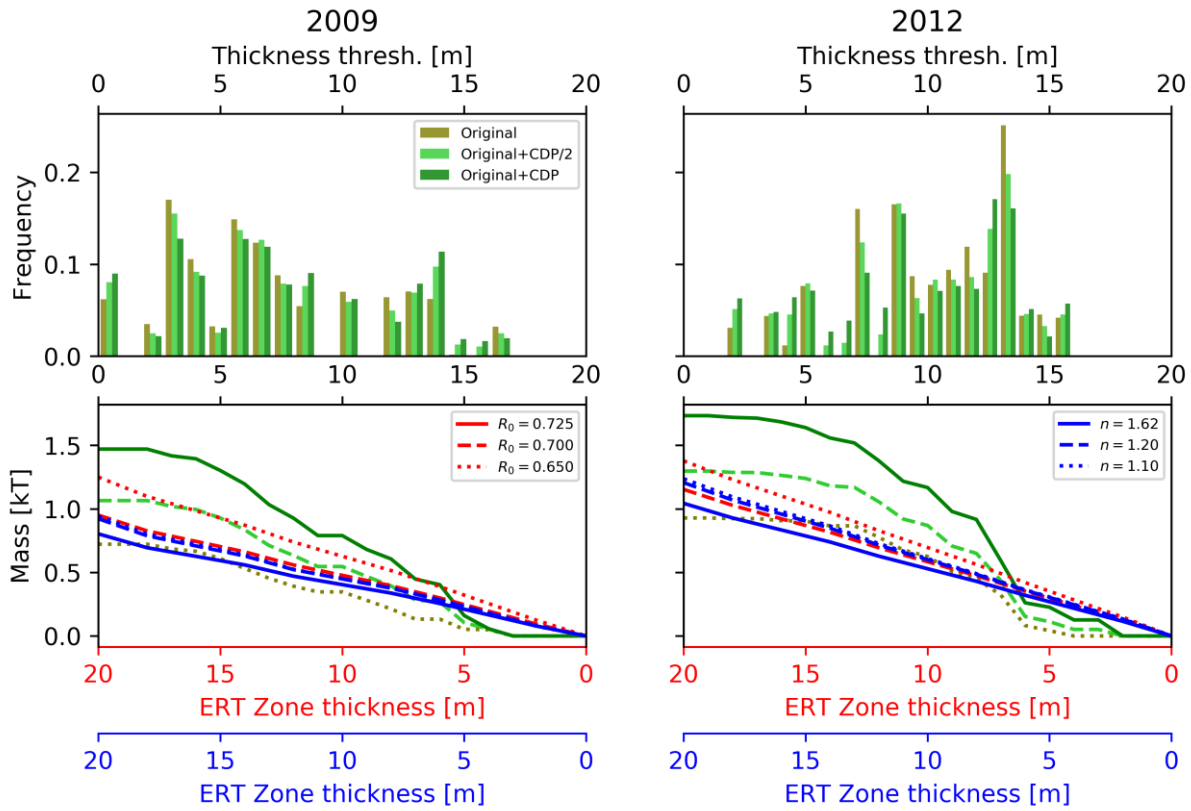

Figure 1: Masses obtained for increasing thickness threshold (seismic) and decreasing zone thickness (ERT).

5. References

Bergmann, P., Diersch, M., Goetz, J., Ivandic, M., Ivanova, A., Juhlin, C., Kummerow, J., Liebscher, A., Lueth, S., Meekes, S. and Norden, B., 2016. Review on geophysical monitoring of CO2 injection at Ketzin, Germany. Journal of Petroleum Science and Engineering, 139, pp. 112-136, https://doi.org/10.1016/j.petrol.2015.12.007

Bergmann, P., Schmidt-Hattenberger, C., Kiessling, D., Rücker, C., Labitzke, T., Henninges, J., Baumann, G., & Schütt, H. (2012). Surface-downhole electrical resistivity tomography applied to monitoring of CO2 storage at Ketzin, Germany. Geophysics, 77(6), B253–B267, https://doi.org/10.1190/geo2011-0515.1

Ivandic, M., Juhlin, C., Lueth, S., Bergmann, P., Kashubin, A., Sopher, D., Ivanova, A., Baumann, G. and Henninges, J., 2015. Geophysical monitoring at the Ketzin pilot site for CO2 storage: New insights into the plume evolution. International Journal of Greenhouse Gas Control, 32, pp. 90-105, https://doi.org/10.1016/j.ijggc.2014.10.015

Ivanova, A., Kashubin, A., Juhojuntti, N., Kummerow, J., Henninges, J., Juhlin, C., Lüth, S. and Ivandic, M., 2012. Monitoring and volumetric estimation of injected CO2 using 4D seismic, petrophysical data, core measurements and well logging: a case study at Ketzin, Germany. Geophysical Prospecting, 60(5), pp. 957-973, https://doi.org/10.1111/j.1365-2478.2012.01045.x

Lüth, S., Ivanova, A. and Kempka, T., 2015. Conformity assessment of monitoring and simulation of CO2 storage: A case study from the Ketzin pilot site. International Journal of Greenhouse Gas Control, 42, pp. 329-339, https://doi.org/10.1016/j.ijggc.2015.08.005

Schmidt-Hattenberger, C., Bergmann, P., Bösing, D., Labitzke, T., Möller, M., Schröder, S., Wagner, F. and Schütt, H., 2013. Electrical resistivity tomography (ERT) for monitoring of CO2 migration-from tool development to reservoir surveillance at the Ketzin pilot site. Energy Procedia, 37, pp.4268-4275, https://doi.org/10.1016/j.egypro.2013.06.329